ANNALS OF GEOPHYSICS, 68, 3, NS336, 2025; doi:10.4401/ag-9203
OPEN ACCESS

A Multi-method Geophysical Approach for Complex Shallow Landslide Characterization

Mohammadyar Rahimi[1], Clinton Wood[*,1], Mersad Fathizadeh[1], Salman Rahimi[2]

(1) University of Arkansas, Civil engineering faculty, Fayetteville, AR, USA
(2) Arup Consulting Engineer, Oakland, CA, USA

Article history: received November 11, 2024; accepted June 30, 2025

Abstract

This case study demonstrates the value of combining multiple non-invasive geophysical methods to characterize a landslide along Highway 7 near Jasper, Arkansas, USA. Geophysical testing was conducted using Multichannel Analysis of Surface Waves (MASW), Horizontal to Vertical Spectral Ratio (HVSR), and Electrical Resistivity Tomography (ERT), supplemented by select soil borings. The geophysical investigation aimed to provide a high-resolution, near-continuous view of subsurface conditions, including bedrock depth and the location of the groundwater table or highly saturated zones within the slide area. These factors are important contributors to slope instability. The MASW results revealed a highly variable depth to weathered bedrock along the observed displacement zone, with the bedrock becoming shallower downslope. The ERT data detected saturated zones associated with observed seeps and springs in the area, which were feeding water into the unstable zone. A low resistivity zone on the north side correlated to wet spots, while south of the highway, saturation occurred near the deeper bedrock interface. Additionally, a grid-based HVSR approach generated a high-resolution image of the shallow and complex bedrock topography across the slide area, providing valuable information for the slope repair design. Overall, the integrated geophysical approach offered a more sustainable, rapid, and cost-effective solution for comprehensive landslide characterization and slope stability assessment, compared to relying solely on conventional methods. The combined geophysical results provided a detailed, high-resolution understanding of the subsurface conditions influential for stability analyses and slope repair design.

Keywords: Landslide; Geophysics; Subsurface Imaging; HVSR; MASW; ERT

1. Introduction

Landslides represent major geologic hazards that incur substantial serviceability issues and economic losses annually across transportation networks, infrastructure, and buildings worldwide (Petley, 2012). Global estimates indicate annual economic losses exceeding $20 billion and thousands of fatalities, particularly in mountainous regions and areas with intense rainfall or seismic activity (Kjekstad and Highland, 2009; Froude and Petley, 2018). In the United States alone, landslides cause approximately $3.5 billion in damage annually, significantly affecting vital transportation infrastructure (Highland and Bobrowsky, 2008). The complex nature of landslides, influenced

by various triggering factors, including precipitation, seismic activity, and human intervention, necessitates comprehensive investigation approaches for effective risk management (Hungr et al., 2014).

Characterizing landslide geometry, hydrogeological regime, movement kinematics, and failure mechanisms constitutes an essential step for hazard analysis, monitoring, remediation, and mitigation measures (Jongmans and Garambois, 2007). Traditional site investigation techniques, primarily relying on boreholes and in-situ testing while providing detailed point-wise information, are often costly and time-consuming. Moreover, these conventional methods provide only discrete subsurface data at isolated locations that fail to capture the innate 3D complexities of many landslides tied to slope morphology, geology, hydrology, and seismology. In challenging terrains, particularly those with steep slopes or active movement, conventional investigation methods may be impractical or pose significant safety risks to investigation personnel (Whiteley et al., 2019).

Recent advances in non-invasive geophysical methods have revolutionized landslide investigation by providing rapid wide-area scanning tools to image landslide structures at higher resolutions critical for predictive modeling. These methods offer cost-effective alternatives while maintaining investigation quality and significantly reducing environmental impact (Pazzi et al., 2019). Seismic methods like Multichannel Analysis of Surface Wave (MASW) have been employed to determine the subsurface layering and soil/rock interface, elastic dynamic properties, and stiffness variations indicative of slip surface geometry (Harba, 2019; Hussain et al., 2020; Rahimi et al., 2021). MASW's ability to detect variations in shear wave velocity makes it particularly suitable for identifying potential failure surfaces and zones of weakness within the slope.

Electrical Resistivity Tomography (ERT) has emerged as a powerful tool to map stratigraphic information, soil type, internal seepage pathways, and variable saturation zones, leading to separation between moving soil material and below more stable hard rock (Samodra, 2020; Imani et al., 2021; Rahimi et al., 2024a). ERT sensitivity to moisture content variations makes it especially valuable for understanding hydrogeological conditions that often trigger or accelerate landslide movement (Chambers et al., 2011). Ambient vibration techniques such as Horizontal-to-Vertical Spectral Ratio (HVSR) can estimate soil thickness overlaying bedrock as complementary information governing failure plane development, particularly for landslides with shallow bedrock (Alonso-Pandavenes, 2023; Ávila-Barrientos, 2023). Moreover, ambient noise techniques are proposed for their ability to assess near-surface conditions and refine subsurface velocity models (D'Amico et al., 2019). The passive nature of ambient noise measurements makes it particularly suitable for urban environments where active seismic methods should be complemented.

The integration of multiple geophysical datasets provides improved subsurface constraints to overcome individual limitations and ambiguities (Bichler et al., 2004; Pazzi et al., 2019; Rahimi et al., 2024b). Recent case studies further illustrate the potential of integrated approaches; for example, the integration of active and passive seismic imaging techniques has been shown to robustly delineate subsurface shear-wave velocity structures in landslide-affected areas (Chávez-García et al., 2021), while coupling seismic refraction with ambient noise tomography effectively identifies low-velocity zones associated with landslide-prone materials (Cárdenas-Soto et al., 2024). Joint structural models better inform slope stability analyses by reducing reliance on sparse direct sampling and providing complementary information about different physical properties of the subsurface materials. When combined with targeted conventional investigation methods, this multi-method approach offers a more comprehensive understanding of landslide mechanisms and behavior (Whiteley et al., 2019).

This study demonstrates the value of a combined MASW, ERT, and HVSR geophysical approach, verified with a limited borehole investigation, for comprehensive landslide characterization through a case study along Highway 7 near Jasper, Arkansas. The investigation aimed to provide a high-resolution image of bedrock morphology, hydrogeology, and saturated zones contributing to the slope failure. In this context, the term high-resolution refers to the improved interpretive capability achieved through the integration of complementary geophysical methods. Specifically, ERT is particularly effective in detecting saturated zones and seepage pathways, while seismic methods such as MASW and HVSR contribute critical information on variations in bedrock depth and the distribution of weathered material. This integrated approach offers a more complete and detailed subsurface characterization than single method alone, providing valuable support for hazard mitigation planning in landslide-prone areas.

2. Site location and geology

The investigated slope is located along Arkansas Highway 7 near Jasper, Newton County, Arkansas, within the Salem Plateau region of the Ozark Highlands physiographic province (Adamski et al., 1995). The Ozark Highlands,

a distinctive physiographic region encompassing approximately 75,000 square kilometers across southern Missouri, northern Arkansas, northeastern Oklahoma, and southeastern Kansas, represents one of the most extensive uplifted plateau regions in the central United States. This province formed through the uplift of a broad asymmetrical dome during the Ouachita orogeny in the early to middle Paleozoic Era, with subsequent periods of erosion and denudation shaping its current landscape.

The Salem Plateau lithological framework consists predominantly of nearly horizontal sedimentary bedrock layers, including limestone, dolomite, sandstone, and shales that gently dip away from the St. Francois Mountains toward the Arkansas River Valley (Braden, 2015). These Paleozoic sequences, particularly the carbonate units, have undergone extensive weathering and dissolution, resulting in a mature topography characterized by open ridges divided by steep V-shaped valleys (Adamski et al., 1995). The local geology reflects the broader regional patterns but exhibits specific characteristics that influence slope stability. Soils in the study area are generally thin, consisting of stony residuum weathered from the underlying bedrock. The presence of rock fragments within the soil matrix, derived from the weathering of shale and sandstone, creates heterogeneous soil properties that can affect slope stability and groundwater movement.

The immediate study area exhibits variable slope angles, with the primary slope orientation running approximately from north to south. This study was prompted by the observation of a distress crack in the highway pavement, oriented almost parallel to the primary slope direction. This crack pattern, as shown in Fig. 1, suggests potential deep-seated movement rather than shallow surficial sliding, as the crack orientation aligns with typical tension crack patterns observed in rotational failures (Cruden and Varnes, 1996).

Figure 1. A sample longitudinal crack observed on the pavement.

3. Geophysical investigations

A comprehensive geophysical investigation program was implemented to characterize subsurface conditions potentially contributing to pavement distress and slope instability. The investigation combined three complementary geophysical methods including MASW, HVSR, and ERT. P-wave refraction is also an effective method in geophysical studies for mapping subsurface layers and identifying the boundary between soil layers and the bedrock. However, at this study site, the P-wave velocities of the rock and the water-saturated zones were quite similar. This lack of significant velocity contrast prevents clear identification of the bedrock interface, thereby reducing the method's effectiveness for this specific site.

The surveys were conducted along multiple transects oriented both perpendicular and parallel to the slope to capture the three-dimensional variability of subsurface conditions. Field measurements were conducted over four days (February 1 and 5, 2021; March 8 and 10, 2021) with consistently moist ground conditions and no significant precipitation recorded in the days immediately preceding the surveys. This temporal consistency in ground

moisture conditions helped minimize variations in geophysical measurements that could result from changing subsurface water content. The investigation layout comprised three MASW survey lines, five ERT survey lines, and approximately 100 HVSR measurement points distributed in a grid pattern across the study area, with a particular focus on the apparent slide zone.

Four geotechnical boreholes (B1-B4) were drilled at strategic locations across the site to provide ground-truth validation of the geophysical data. However, boreholes B1 and B3 were positioned outside the primary geophysical survey area and, therefore, could not be directly incorporated into the 2D cross-sectional analyses. Figure 2 presents the spatial distribution of all investigation points, including the geophysical survey lines, HVSR measurement locations, and borehole positions. The figure also illustrates the location of the observed pavement distress crack and the interpreted direction of landslide movement, providing crucial context for understanding the relationship between surface manifestations and subsurface conditions.

The investigation design considered several factors:

1) Survey line orientations were selected to intersect both the observed pavement crack and the suspected slide mass
2) HVSR measurement spacing was optimized to capture variations in bedrock depth while maintaining practical field efficiency
3) ERT line lengths and electrode spacings were chosen to achieve sufficient depth penetration while maintaining a resolution appropriate for detecting potential slip surfaces
4) MASW line positions were selected to provide optimal signal quality while avoiding noise sources such as traffic vibrations.

The specific acquisition parameters, data processing workflows, and quality control measures implemented for each geophysical method are detailed in the following sections, along with the integration approach used to combine these complementary datasets.

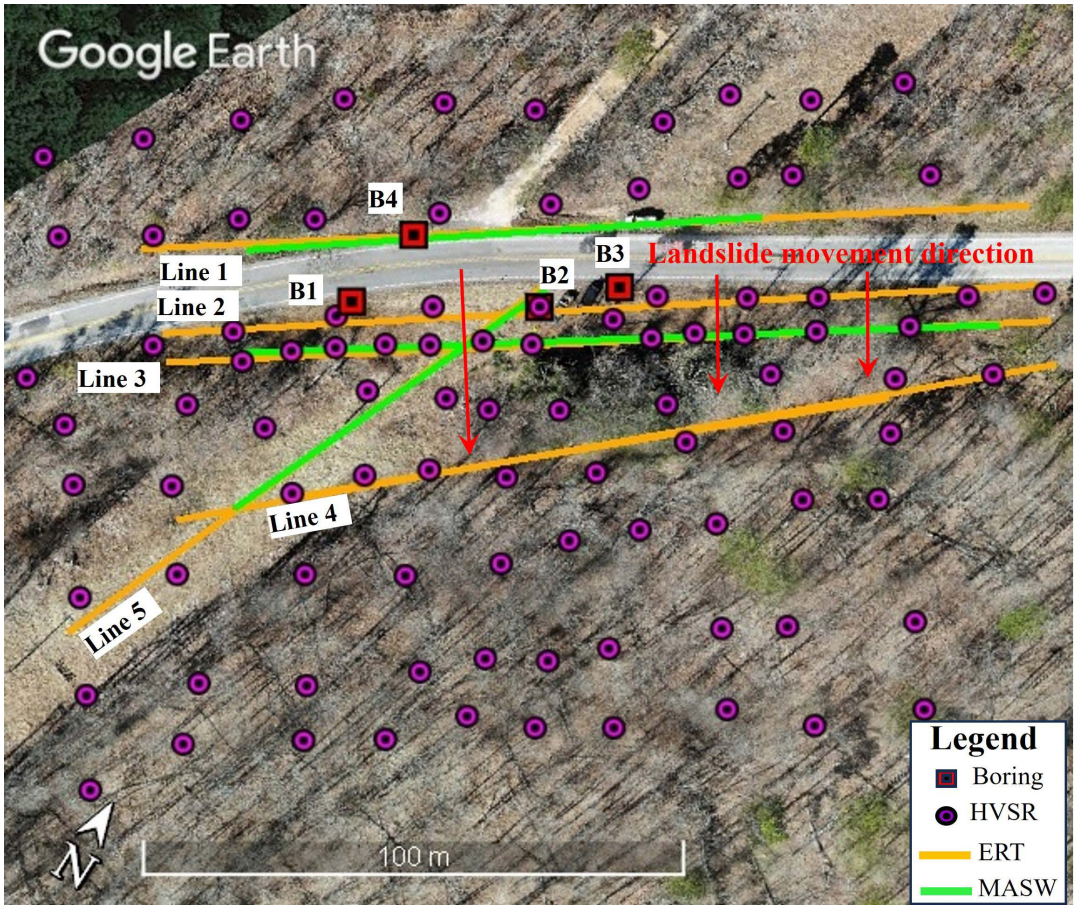

Figure 2. Geophysical field measurement layout.

3.1 MASW measurements

MASW surveys were conducted using a linear array of 48 vertical geophones with a natural frequency of 4.5 Hz. Geophone spacing was adapted to site conditions and survey objectives, with 1 m spacing used for lines parallel to the slope and 2 m spacing for perpendicular lines. Data acquisition employed a roll-along technique to achieve continuous coverage along each survey line. Surface waves were generated using a 5.4 kg sledgehammer striking an aluminum plate coupled to the ground through a rubber damping pad to optimize signal quality and frequency content.

To enhance data quality and reliability, a minimum of three hammer blows were stacked at each source location to improve the signal-to-noise ratio. The source layout was designed to optimize both near-field and far-field effects, with waves generated at 17 distinct offset positions for each array setup. These included positions 1 m beyond each end of the array and at 6 m intervals along the array length. This comprehensive source-offset approach served multiple purposes by minimizing uncertainties in fundamental mode identification, enabling the generation of multiple shear wave velocity profiles for each array setup, providing redundancy in the dataset to assess measurement consistency, and allowing evaluation of near-field effects on the recorded wavefields.

Data processing was performed using a sliding window approach, where multiple 24-geophone subarrays were extracted from the full 48-geophone spread. These subarrays were analyzed sequentially to generate a pseudo 2D shear wave velocity (Vs) cross-section along each survey line, following the methodology outlined by (Rahimi et al., 2019; Yust et al., 2024). The raw dispersion data from multiple source offsets were processed using the frequency domain beamformer method (Zywicki and Rix, 1999) implemented in MATLAB. This method offers several advantages over traditional f-k analysis, particularly in handling non-uniform ambient noise and providing better resolution at lower frequencies.

The dispersion curve extraction process involved combining data from multiple source offsets to enhance signal quality, followed by automated picking of maximum spectral peaks in the frequency-wavenumber domain to minimize user bias. This was complemented by careful identification and isolation of the fundamental mode of Rayleigh wave propagation, and assessment of dispersion curve uncertainty using the multiple sources offset data. The experimental dispersion data consistently showed dominant fundamental mode energy across the frequency range of interest (typically 5-50 Hz). Figure 3a presents a representative experimental dispersion image showing the energy distribution in the frequency-phase velocity domain while Fig. 3b displays the extracted fundamental mode dispersion curve used for subsequent inversion. The experimental dispersion data consistently showed dominant fundamental mode energy across the frequency range of interest, typically between 5 and 50 Hz. Above 50 Hz the curve flattens, indicating limited sensitivity to shallow, thin layers. This behavior is consistent with the relatively simple subsurface conditions at the site, where limited lateral and vertical variability is observed in the upper layers. As a result, the inversion was focused on capturing the dominant velocity contrast associated with the transition from unconsolidated materials to weathered bedrock.

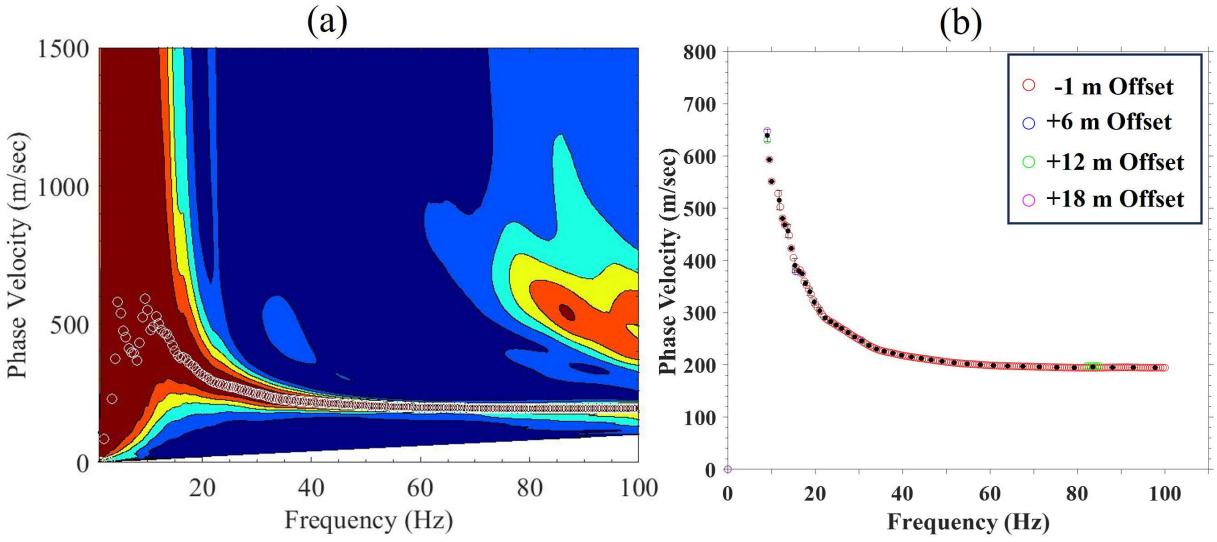

Figure 3. Typical experimental dispersion data points (a) raw and (b) refined.

The inversion process was performed using the Geospy software package, incorporating both the Rayleigh wave dispersion data and the peak frequency from corresponding HVSR measurements. The inversion parameterization was guided by available borehole information to constrain the layer geometry and expected velocity ranges. The process employed a probabilistic approach to account for uncertainties in both the dispersion and HVSR data. To generate the final pseudo 2D Vs cross-sections, the individual 1D ≠ profiles from each subarray were combined using a spatial averaging approach designed to account for the overlapping nature of adjacent measurements This process helped ensure smooth transitions between adjacent 1D profiles while maintaining fidelity to the measured data.

3.2 ERT measurements

ERT surveys were conducted along five strategic survey lines, comprising four lines oriented perpendicular to the slide direction and one parallel line. Data acquisition was performed using an Advanced Geosciences Inc. (AGI) SuperSting R8/IP WiFi resistivity meter, a multi-channel system capable of simultaneous measurements across multiple electrode pairs. The moist ground conditions during testing ensured good electrode coupling and low contact resistance, which are crucial factors for high-quality resistivity measurements.

The survey design utilized 56 surface electrodes for each survey line, with electrode spacing optimized based on the required depth of investigation and desired resolution. Two configurations were employed including a 2 m spacing yielding a total array length of 110 m and a 3 m spacing extending to 165 m. This dual-spacing approach allowed for both detailed shallow imaging and deeper penetration where needed. The surveys employed a combination of dipole-dipole and strong gradient array configurations to maximize data coverage and resolution. The strong gradient array, an optimized configuration derived from traditional Wenner and dipole-dipole arrays, was particularly effective in providing balanced sensitivity to both vertical and horizontal resistivity variations, which is essential for identifying potential slip surfaces and stratigraphic boundaries.

Precise spatial control was maintained throughout the surveys using a dual-positioning approach. A Nikon Total Station was employed to survey the relative positions and elevations of individual electrodes along each profile, while a Trimble Geo7x centimeter-accuracy GPS unit was used to establish absolute coordinates for the profile endpoints. This detailed positional data was crucial for accurate topographic corrections and integration with other geophysical datasets.

Data processing and inversion were performed using AGI's EarthImager2D software package, incorporating the surveyed electrode elevations to account for topographic effects on the measurements. The inversion process employed a robust least-squares optimization approach to minimize the differences between measured and calculated apparent resistivity values. Quality control measures included rigorous data filtering based on measurement repeatability and reciprocal error analysis. The root mean square error (RMSE) between measured and modeled resistivity values was used as the primary quality metric, with all final inversions achieving RMSE values below 5% after multiple iteration trials. This level of fit was achieved through careful data editing, which involved removing up to 20% of the measured data points that showed excessive noise or inconsistency with neighboring measurements.

The inversion parameters were carefully selected to balance the competing demands of fitting the observed data while maintaining geologically reasonable models. Smoothness constraints were applied to prevent the development of unrealistic sharp boundaries while still allowing the detection of significant resistivity contrasts associated with geological or hydrogeological features. The resulting resistivity models provide detailed images of the subsurface resistivity distribution, with resolution gradually decreasing with depth as expected for surface-based electrical measurements.

The combination of careful survey design, precise positioning, and rigorous data processing resulted in high-quality resistivity models that effectively delineate variations in subsurface materials and moisture content. These models provide key information about the internal structure of the landslide, particularly regarding the distribution of water-bearing zones and potential slip surfaces.

3.3 HVSR measurements

HVSR measurements were conducted using Nanometrics Trillium Compact seismometers, sophisticated three-component instruments featuring a flat frequency response from 100 Hz to 20 seconds. This broad bandwidth ensures

accurate recording of ambient vibrations across frequencies relevant to both shallow and deeper geological structures. Each measurement station was recorded for a minimum duration of 15 minutes to ensure the statistical reliability of the spectral estimates. The measurements were systematically collected along the MASW and ERT survey lines and extended into a grid pattern covering the entire slide area to provide comprehensive spatial coverage of the site.

Data processing followed the rigorous guidelines established by the Site Effects Assessment using Ambient Excitations (SESAME, 2004) project. These guidelines provide specific criteria for evaluating the reliability and clarity of HVSR peaks, including requirements for peak amplitude, standard deviation, and stability across different time windows. Only peaks meeting these stringent criteria were considered valid indicators of significant subsurface impedance contrasts and used in subsequent analyses.

For measurements exhibiting clear and reliable peaks, the depth to the primary impedance contrast (typically representing the interface between softer soil materials and stiffer bedrock) was estimated using the fundamental relationship:

$$H = \frac{V_{s,\text{avg}}}{4f} \tag{1}$$

where:
H represents the thickness of sediments above the impedance contrast
$V_{s,\text{avg}}$ is the average shear wave velocity of materials above the impedance contrast
f denotes the frequency associated with the HVSR peak

The average shear wave velocity ($V_{s,\text{avg}}$) values used in this equation were derived from the MASW testing results, providing a consistent integration between the two methods. This approach was preferred over back-calculation from boring information as it offers more spatially continuous data and better represents the dynamic properties of the subsurface materials. The combination of HVSR peak frequencies and MASW-derived velocities allowed for estimation of bedrock depths across the study area. The spatial distribution of HVSR measurements enabled the development of a detailed 3D representation of the bedrock surface, particularly valuable in areas between the primary geophysical survey lines.

4. Results

The results of the MASW and ERT surveys along with the HVSR recordings are presented in this section.

4.1 MASW result

Figure 4 presents the pseudo 2D shear wave velocity (Vs) cross-sections for survey lines 1 and 3, accompanied by an orthomosaic image of the slide area and the soil stratigraphy from borings B2 and B4. The pseudo 2D Vs cross-sections were generated by interpolating and combining individual 1D Vs profiles. The pseudo 2D Vs cross-section for Line 1 reveals two distinct geologic units. The upper layer consists of medium dense to very dense soils/highly weathered rock, characterized by Vs values typically ranging from 350-600 m/s. This layer demonstrates a thickness varying from 10-12 m. Below this lies a competent weathered rock unit that exhibits Vs values between 650-1100 m/s, showing a clear velocity contrast with the upper layer and corresponding to the weathered rock encountered in boring logs. The interface between these units, marked by a solid black line in Fig. 4, shows remarkable consistency in depth of the survey line, getting slightly shallower toward end of the line. The slight discrepancy between MASW-derived depths and borehole B4 observations can be attributed to topographic effects, specifically the elevation difference between the MASW array location (positioned in the highway north ditch) and boring B4. Additionally, stratigraphic complexity plays a role, as evidenced by the presence of a thin clay layer between highly weathered and weathered shale in B4, which falls below the vertical resolution capability of the MASW method (Foti et al., 2018).

The subsurface structure along Line 3 similarly exhibits a two-layer system. The upper layer comprises medium dense to very dense soils/highly weathered rock, with consistent Vs values around 350 m/s and thickness varying between 9-12 m. This is underlain by a competent rock unit with Vs ranging from 650-1000 m/s, showing strong

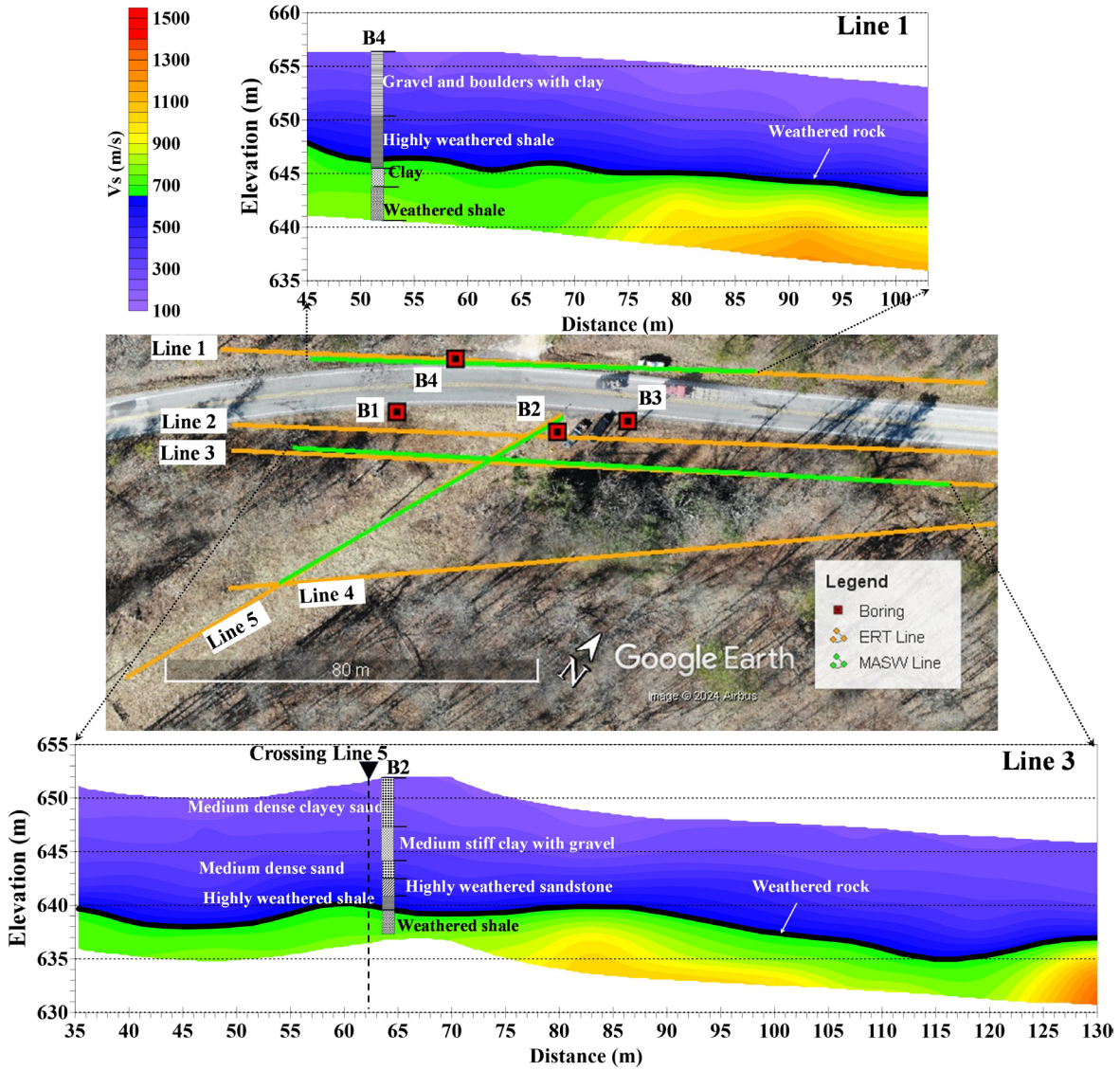

Figure 4. Pseudo 2D Vs cross-sections from MASW for survey lines 1 and 3, along with an orthomosaic image of the slide area and information from the borings B2 and B4.

correlation with weathered rock in boring logs. The depth to the competent rock unit maintains a relatively consistent profile (10-12 m bgs) throughout most of the survey line, with a slight decrease in depth toward the end of the survey line. This pattern mirrors the observations from Line 1, suggesting a systematic geological structure across the site.

The interface between the upper and lower layers proves particularly significant for understanding the slope failure mechanism. Analysis of inclinometer data from boring B2 (Fig. 5a and b), compared with nearby 1D Vs profiles, reveals a good correlation between the zone of displacement (depth <11 m) identified in inclinometer readings and the sharp increase in Vs values associated with the weathered rock unit. This correlation suggests that the slip surface develops preferentially along the interface between the weaker upper materials and the more competent weathered rock unit. Similar relationships between shear wave velocity contrasts and landslide slip surfaces have been documented in other case studies (Pazzi et al., 2019).

As shown in Fig. 6, survey Line 5 exhibits a similar two-layer stratigraphy, with distinct variations in layer geometry that provide crucial insights into the site's geologic structure and stability conditions. The upper layer consists of medium dense to very dense soils and highly weathered rock, underlain by a more competent weathered rock unit as confirmed by boring data. The interface between these units shows significant spatial variability along the survey line, providing information about the site's geomorphological evolution and potential failure mechanisms. From the line origin to approximately 60 m distance along the line, the weathered rock interface maintains a relatively consistent depth of 7.5 m below ground surface (bgs). Beyond this point, a notable deepening of

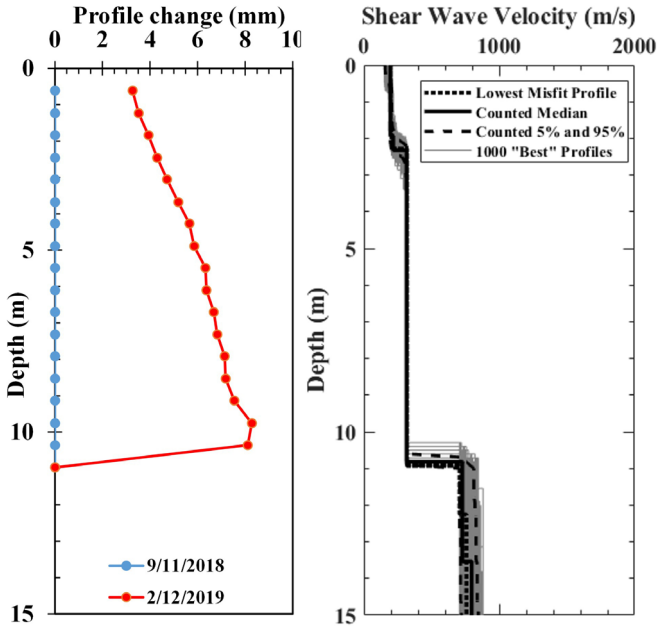

Figure 5. Comparison of the inclinometer readings and 1D Vs profile. (a) Inclinometer readings at B2, blue readings on September 11, 2018, and red readings on February 12, 2019, (b) An example 1D Vs profile from a location close to B2.

the interface occurs, with depths varying between 10-13 m toward the end of the line. This progressive deepening of the weathered rock surface moving upslope likely reflects the combined effects of differential weathering processes and erosional patterns. The systematic variation in bedrock depth observed along Line 5 is particularly significant as it represents a cross-section parallel to the slope direction, thereby capturing the full expression of stratigraphic variations that may influence slope stability.

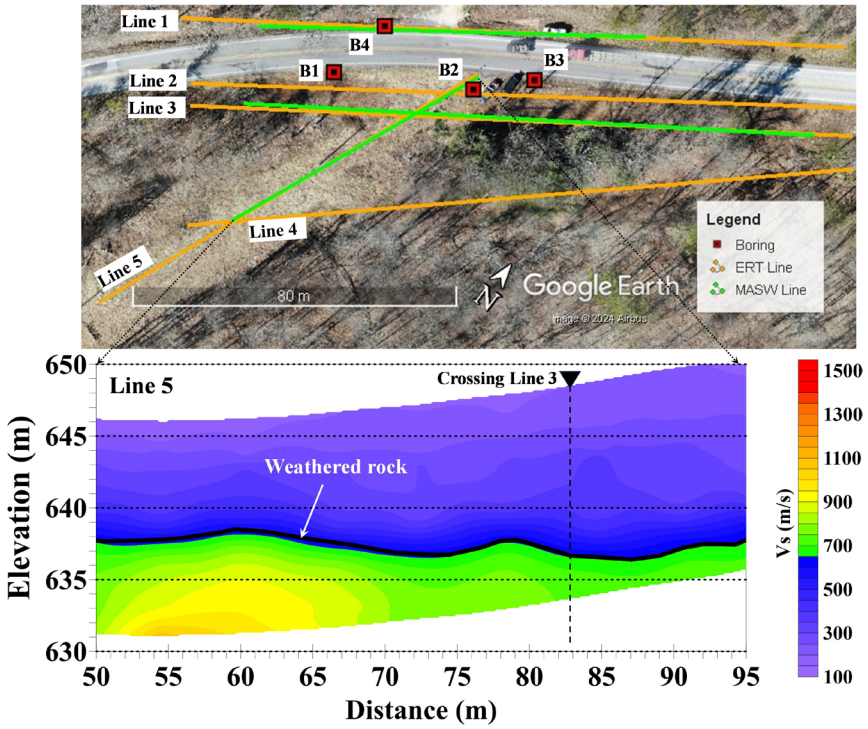

Figure 6. Pseudo 2D Vs cross-sections from MASW for survey Line 5, along with orthomosaic image of the slide area and information from the borings B2 and B4.

The observed pattern of increasing depth to competent rock toward the end of survey line suggests enhanced weathering and erosion of the bedrock in this zone. This interpretation is supported by similar observations in other landslide-prone areas where preferential weathering along discontinuities often creates zones of weakness that can facilitate slope movement (Jaafari, 2024). The increasing depth to competent rock may create conditions favorable for groundwater accumulation and the development of elevated pore pressures, which are known to contribute to slope instability (Whiteley et al., 2019). Furthermore, the irregular bedrock surface could create preferential pathway for groundwater flow and influence the development of potential slip surfaces. The insights gained from Line 5 underscore the importance of conducting geophysical surveys along critical cross-sections that capture the full range of subsurface variability. Accounting for these bedrock depth changes and incorporating the spatial variability into slope stability models could improve prediction of unstable areas.

4.2 ERT result

The results of the ERT surveys are presented as 2D resistivity cross-sections in Fig. 7 for survey Lines 1-4, with Line 5 results shown separately in Fig. 8. For Lines 1 and 3, the weathered rock unit boundaries identified from MASW measurements are superimposed on the resistivity plots to facilitate integrated interpretation. The figure includes vertical guidelines (shown as black and red dashed lines) marking the survey line extents and locations of observed wet spots and springs. Lines 1-4 are presented together due to their similar array lengths (~165 m) and spatial positions. The primary objective of the ERT investigation was to delineate the water table and identify zones of high saturation within the slide mass.

The 2D resistivity profile for Line 1 reveals a pronounced low-resistivity anomaly (<80 Ohm-m), indicated by light and dark purple coloring, extending from approximately 30-60 m along the line. This zone begins near the surface (0-2 m depth) and penetrates to approximately 20 m below ground surface. According to Mauritsch et al. (2000), these low resistivity values typically indicate water-saturated zones in similar geological settings. This low-resistivity zone traverses both soil layers and the weathered rock unit, suggesting either water-filled fractures within the shale bedrock or similar electrical properties between the saturated soil and shale materials. The spatial correlation between this zone and two wet spots/seeps observed at the surface, as documented in the orthomosaic image, provides ground truth validation of the geophysical interpretation. An additional, smaller low-resistivity anomaly appears between 90-110 m along the survey line at depths of 6-15 m, likely representing perched water at or slightly penetrating the bedrock interface.

Line 2, positioned adjacent to the highway's south side, exhibits a distinct low-resistivity zone at an approximate distance of 85-105 m at depths of 13-23 m. Line 3, offset 12 m further south, shows a remarkably similar pattern with a low-resistivity zone (light and dark purple) from 80-105 m horizontally at depths of 10-25 m. The spatial consistency of these anomalies between adjacent survey lines strengthens the interpretation of their significance. Furthermore, these zones demonstrate strong spatial correlation with multiple wet spots and springs observed downslope on the highway's south side, as evidenced in the orthomosaic imagery (Fig. 7).

The resistivity profile for Line 4 reveals an extensive low-resistivity anomaly spanning approximately 70 m along the line (from 45-115 m) and extending from 15-35 m depth. This substantial feature aligns well with two documented springs and wet spots at the slope base. Notably, the elevation of the observed springs (approximately 630 m) corresponds with the upper boundary of the low-resistivity zone, suggesting a potential hydrogeological connection. The survey also detected several smaller, near-surface low-resistivity zones from approximately 70 m to the end of line, indicating possible shallow groundwater pathways or perched water tables. The integration of ERT results with surface observations and MASW data provides a comprehensive understanding of the site hydrogeological conditions. The consistent spatial correlation between geophysically-detected low-resistivity zones and observed surface water features validates the interpretation methodology and supports the use of integrated geophysical approaches for landslide investigation (Whiteley et al., 2019).

The 2D resistivity profile for survey Line 5, presented in Fig. 8, provides instructive insights into the subsurface hydrology of the landslide site. Conducted approximately along a South-North orientation, this survey line traverses the slide area and reveals a complex pattern of low-resistivity zones that demonstrate significant spatial variability in depth and distribution. The survey line is characterized by extensive low-resistivity zones (indicated by light and dark purple coloration) that extend almost continuously along its entire length. However, the depth of these zones exhibits pronounced variations. From the start of the survey line to approximately 50 m, low-resistivity zones are

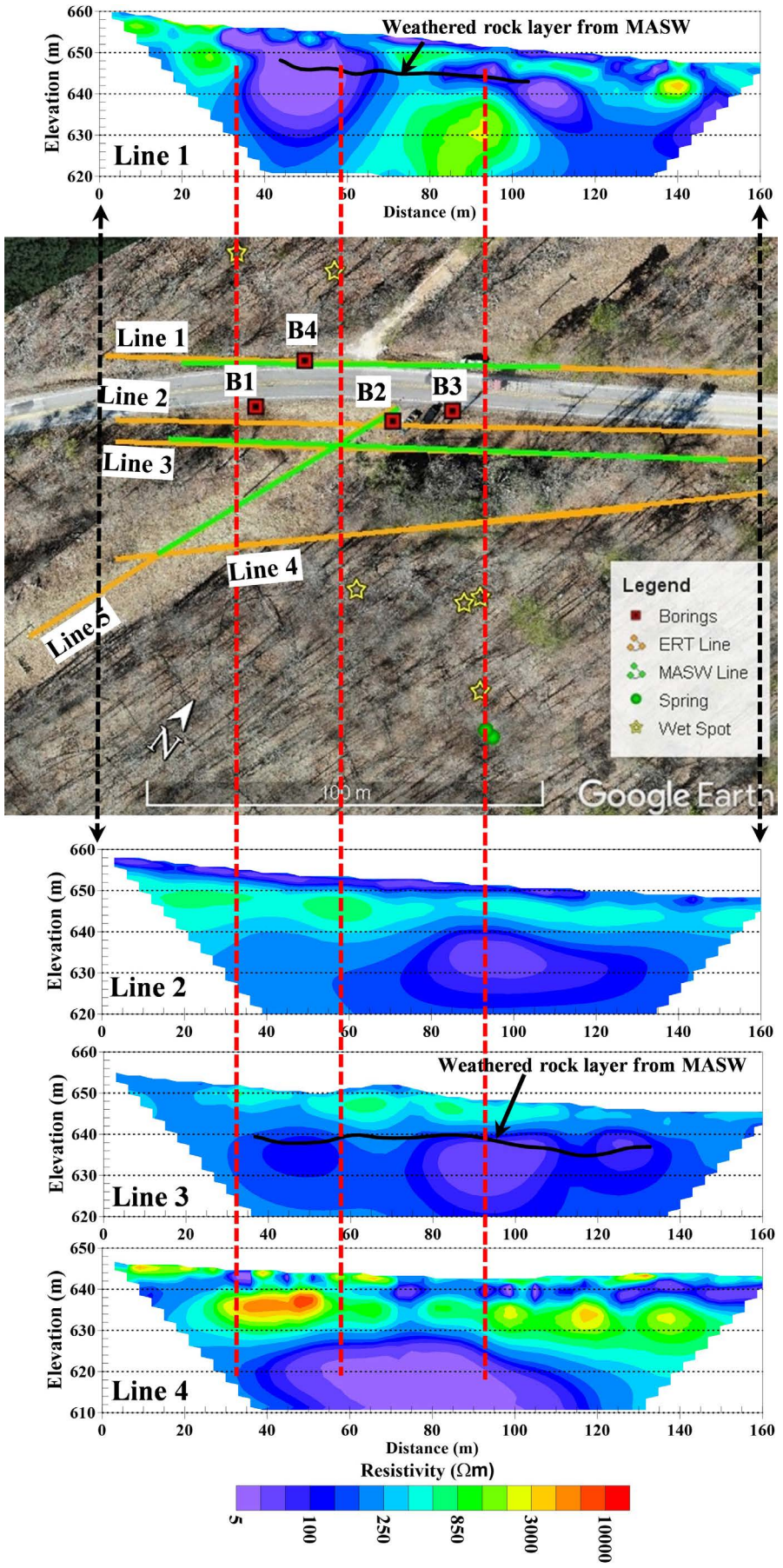

Figure 7. 2D resistivity profiles for Lines 1-4. The black line is the weathered rock unit boundaries identified with the MASW method.

observed at depths ranging from 5-15 m. Beyond the 50 m mark, a notable shift occurs, with the low-resistivity zones deepening to 10-20 m. This systematic deepening of low-resistivity zones moving upslope suggests complex hydrogeological processes influencing water distribution within the slide mass. The depth of these low-resistivity zones demonstrates remarkable correspondence with bedrock depths determined through MASW testing, indicating that these zones are predominantly associated with the weathered rock unit. This correlation supports the interpretation that the low-resistivity anomalies represent water-saturated or highly fractured bedrock zones, a characteristic observation in similar geological settings.

The integrated analysis of ERT surveys across multiple lines reveals distinctive spatial patterns of water saturation. For the north highway alignment (Line 1), the primary low-resistivity zone is predominantly located on the western segment of the survey line. This zone extends from near-surface to significant depths, indicating potential preferential water accumulation and infiltration pathways. In contrast, for the south highway alignment (Lines 2, 3, and 4), the low-resistivity zones are concentrated on the eastern segments. These zones are typically positioned near or below the bedrock elevation, suggesting complex groundwater interactions within the subsurface geological structure. The geophysical findings demonstrate good alignment with field-observed wet spots and springs. This correlation validates the ERT methodology and provides robust evidence of subsurface hydrological conditions contributing to slope instability.

While the ERT measurements offer detailed insights into subsurface water distribution, it is crucial to acknowledge inherent limitations. The depths of these saturated zones are subject to temporal variability, particularly in response to seasonal precipitation patterns. Groundwater levels can fluctuate significantly, potentially altering the observed resistivity patterns throughout the year. The systematic variations in low-resistivity zone depths across different survey lines suggest a complex three-dimensional groundwater system within the landslide. These findings highlight the importance of integrated geophysical approaches in understanding slope hydrology and potential failure mechanisms (Whiteley et al., 2019).

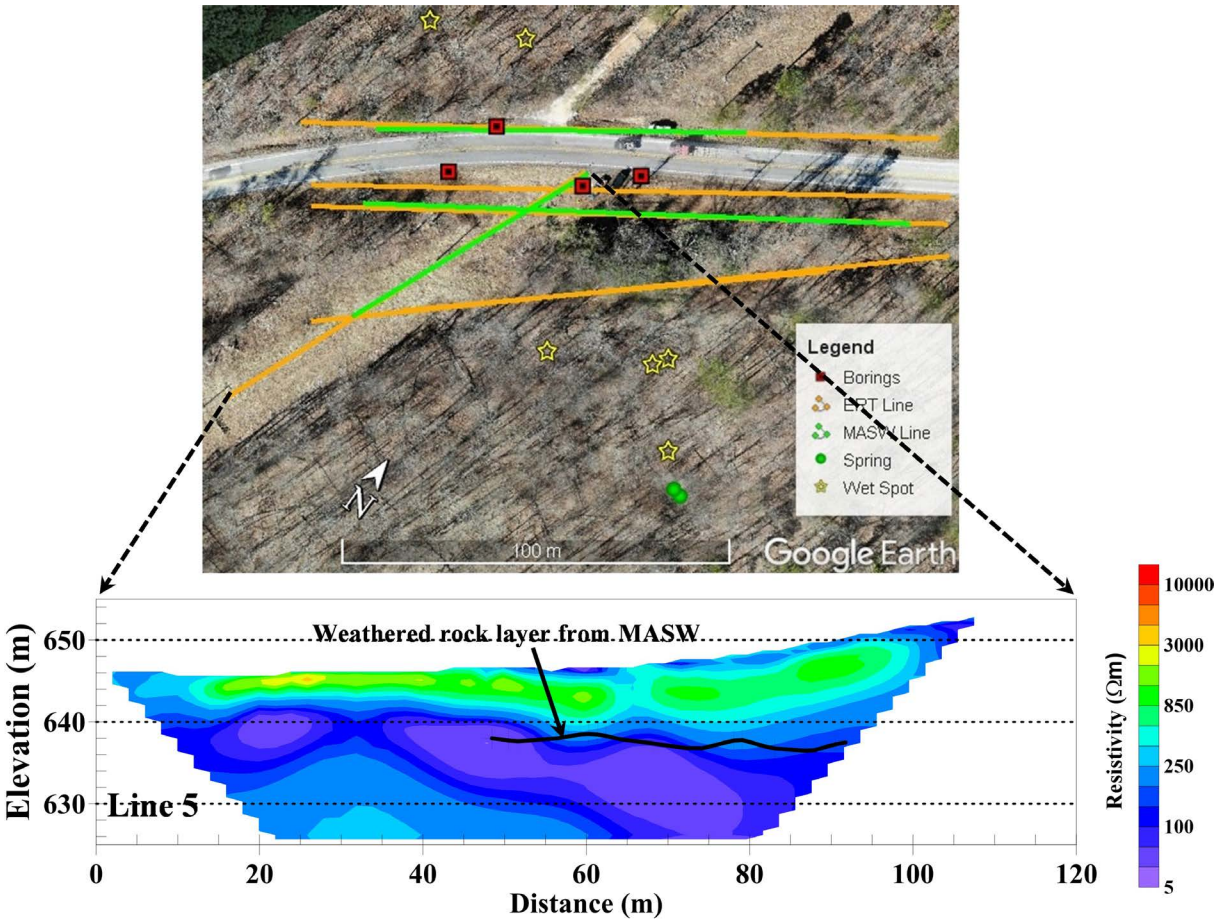

Figure 8. 2D resistivity profiles for Lines 5. The black line is the weathered rock unit boundaries identified with the MASW method.

4.3 HVSR result

A comprehensive network of Horizontal-to-Vertical Spectral Ratio (HVSR) measurements was implemented across the slide area to characterize the spatial variation in weathered rock unit depth. As shown in Fig. 9, the HVSR peak frequencies (F0) obtained at measurement stations ranged from 7.5 to 70 Hz. These frequencies, combined with time-averaged shear wave velocity ($V_{s,avg}$) values derived from MASW measurements, were used to estimate bedrock depth using Eq. (1). The integration of HVSR and MASW data provided robust constraints for generating detailed contour and 3D maps of the weathered rock surface topology. To develop accurate bedrock elevation estimates, surface topography data from GPS and total station surveys were combined with Digital Elevation Model (DEM) information extracted from ArcGIS Online regional maps.

The results of this integrated analysis are presented as a series of contour maps in Fig. 10, displaying surface elevation (a), bedrock elevation (b), and depth to bedrock (c) across the study area. These maps provide

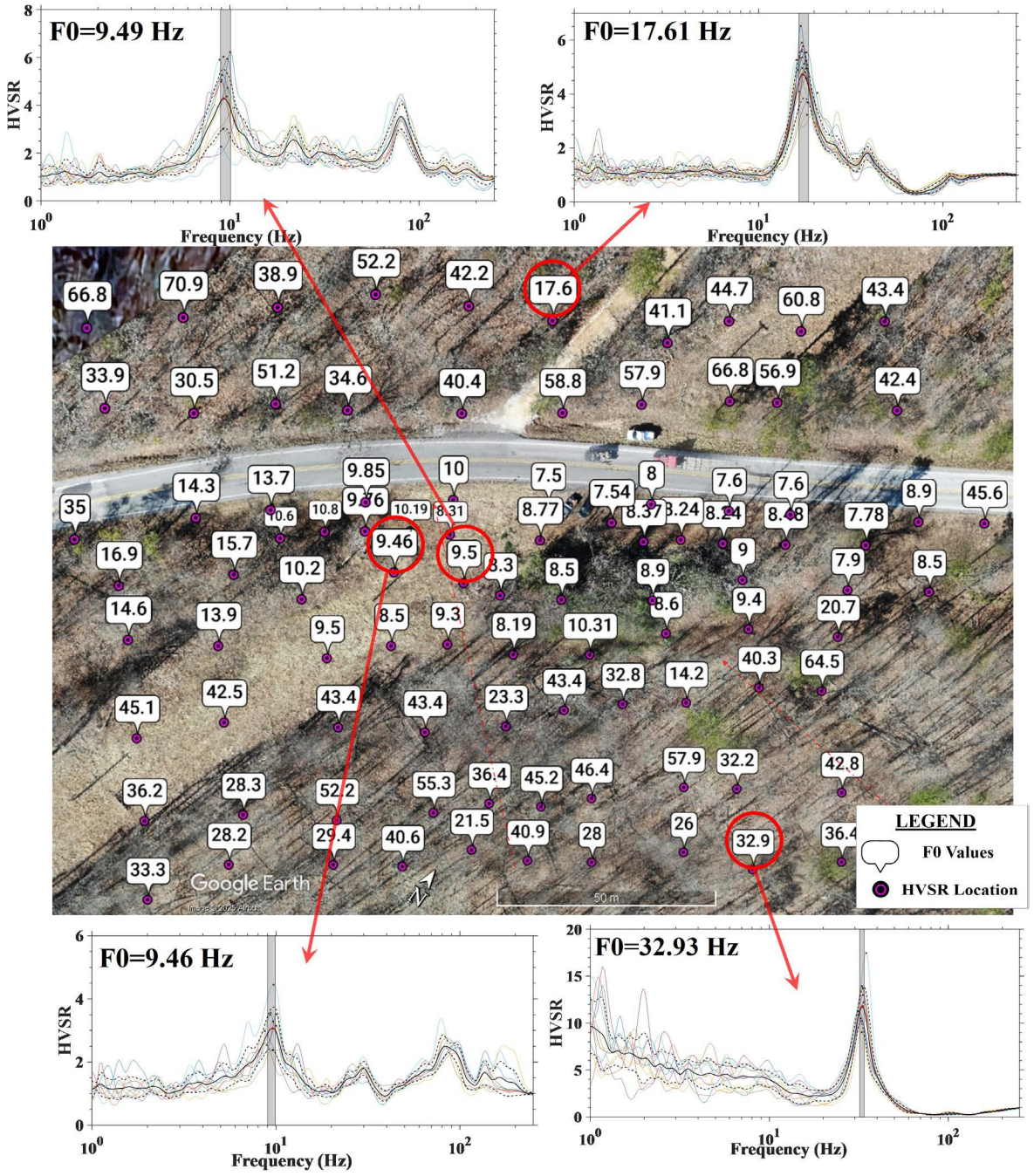

Figure 9. HVSR peak frequencies (F0) and four sample HVSR curves showing frequency peak.

a comprehensive framework for determining bedrock parameters at any location within the slide area. The contour map of bedrock depth (Fig. 10c) reveals a systematic decrease in depth to bedrock moving downslope, a pattern that is further corroborated by the bedrock elevation contours shown in Fig. 10b. To enhance visualization and interpretation of the site subsurface geometry, three-dimensional representations of both surface and bedrock topography were developed. Figure 11a presents the 3D surface elevation map, while Fig. 11b illustrates the corresponding bedrock elevation surface. These complementary visualizations enable detailed analysis of the spatial relationships between surface topography and bedrock morphology throughout the study area. The 3D bedrock elevation map demonstrates that bedrock topography generally mirrors surface topography across much of the slide area. However, notable variations are observed, particularly in the vicinity of the highway alignment where bedrock depth is greatest, gradually decreasing downslope as evidenced in the contour map (Fig. 11b).

The increased thickness of soil and highly weathered rock beneath the highway alignment has significant implications for slope stability. When these materials become saturated, their shear strength typically decreases while their mass increases, potentially amplifying gravitational driving forces that contribute to slope instability. Furthermore, saturation can reduce friction along critical slip surfaces, further compromising slope stability. The detailed characterization of variable soil and weathered bedrock thicknesses achieved through the extensive HVSR measurement campaign provides instructive insights into the distribution of potentially destabilizing masses across the irregular bedrock surface. This comprehensive mapping of subsurface conditions enables more refined stability analyses by accounting for spatial variations in overburden thickness and material properties (Uhlemann et al., 2017). The integration of multiple geophysical methods with traditional surveying techniques has produced a detailed subsurface model that can inform both the understanding of current slope behavior and the design of potential remediation measures. The observed patterns in bedrock topology, particularly the thickening of overburden materials beneath the highway, may play a critical role in the site's hydrogeological regime and overall stability conditions (Del Gaudio et al., 2014).

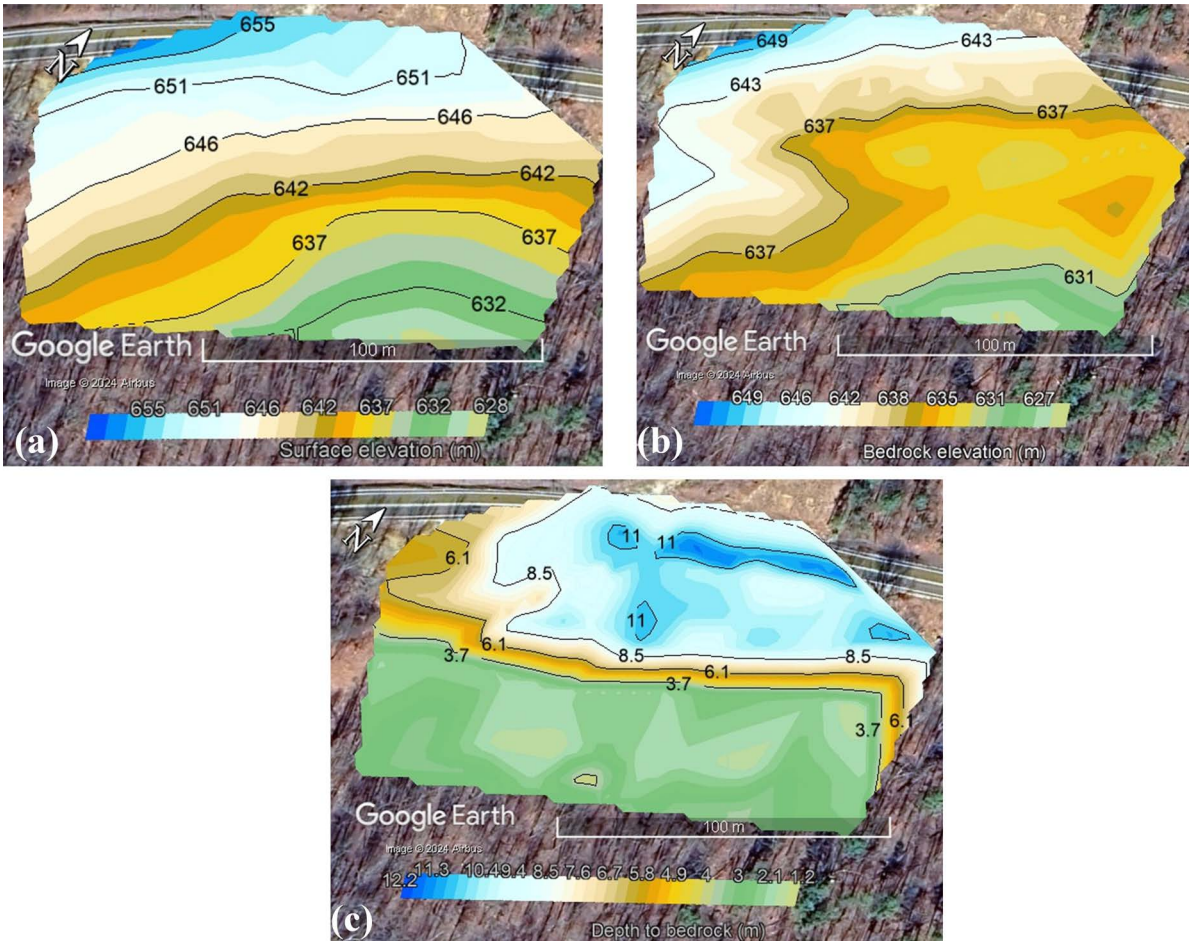

Figure 10. Contour maps of (a) surface elevation, (b) bedrock elevation and (c) depth to bedrock.

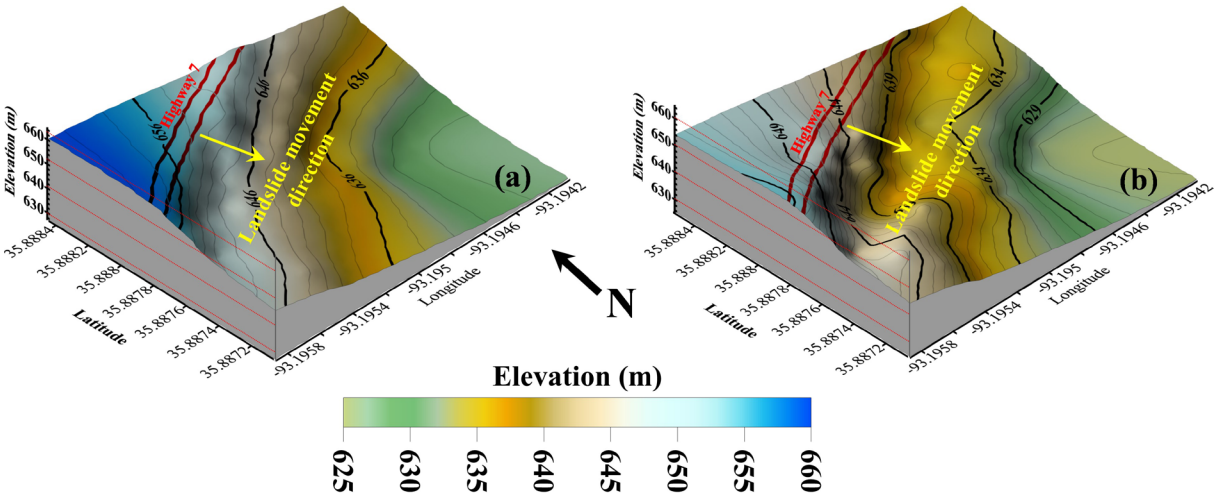

Figure 11. 3D maps for the Jasper slide (a) 3D map of surface elevation, (b) 3D map of bedrock elevation.

5. Conclusions

The multi-method geophysical investigation conducted along the distressed highway segment near Jasper, Arkansas, provided useful insights into the landslide geometry, hydrogeology, and failure mechanisms. The key findings and conclusions from this study are as follows:

- The MASW surveys detected a layered subsurface with an upper zone of medium dense to very dense soils/highly weathered rock underlain by a more competent weathered bedrock unit. The depth to this weathered bedrock interface showed a systematic decrease moving downslope, aligning with inclinometer data to validate the location of the critical slip surface.
- ERT imaging revealed complex patterns of low-resistivity anomalies, indicating the presence of water-saturated zones and potential groundwater pathways within the landslide mass. The spatial distribution and depth variations of these anomalies demonstrated a strong correlation with the irregular bedrock topography mapped by the HVSR measurements.
- The comprehensive HVSR dataset enabled the development of detailed 3D models of the bedrock surface across the study area. These models revealed a systematic deepening of the bedrock interface moving upslope, suggesting preferential weathering and erosion processes that may have contributed to slope instability.
- The integration of these complementary geophysical datasets provided a robust 3D framework for evaluating the complex interplay of subsurface geology, hydrogeology, and slope geometry that enabled the ongoing slope distress. This thorough approach offers significant advantages over traditional borehole-based investigations, which often fail to capture the inherent 3D complexities of landslide systems.

The successful application of this integrated geophysical approach demonstrates its potential for efficient, sustainable, and comprehensive landslide characterization in similar challenging terrain. Future investigations could further benefit from the incorporation of seasonal ERT monitoring, continuous inclinometer and piezometer measurements, and additional hydrogeological assessments to capture the temporal variability of groundwater conditions and their influence on slope stability.

Acknowledgements. The authors are grateful for the financial support provided from ARDOT from the TRC1803 Project. Any opinions, findings, and conclusions or recommendations expressed in this article are those of the authors and do not necessarily reflect the view of the funding agency.

References

Adamski, J. C., J. C. Petersen, D. A. Freiwald and J. V. Davis (1995). Environmental and hydrologic setting of the Ozark Plateaus study unit, Arkansas, Kansas, Missouri, and Oklahoma, Water-Resources Investigations Report, 94, 4022, U.S. Geological Survey, doi:10.3133/wri944022.

Alonso-Pandavenes, O., F. J. Torrijo, J. Garzón-Roca and A. Gracia (2023). Early investigation of a landslide sliding surface by HVSR and VES geophysical techniques combined, a case study in Guarumales (Ecuador), Appl. Sci., 13, 2, 1023, doi:10.3390/app13021023.

Ávila-Barrientos, L., L. A. Yegres-Herrera and H. Flores-Estrella (2023). Characterization of landslides in Federal Highway 1D, Baja California, Mexico, using seismic noise records and the HVSR method, Nat. Haz., 1-19, doi:10.1007/s11069-023-06053-3.

Braden, A. K. (2015). Geologic map of the Mt. Judea quadrangle, Newton County, Arkansas, Arkansas Geological Commission.

Chambers, J. E., P. B. Wilkinson, O. Kuras, J. R. Ford et al. (2011). Three-dimensional geophysical anatomy of an active landslide in Lias Group mudrocks, Cleveland Basin, UK, Geomorphology, 125, 4, 472-484, doi:10.1016/j.geomorph.2010.09.017.

Bichler, A., P. Bobrowsky, M. Best, M. Douma et al. (2004). Three-dimensional mapping of a landslide using a multi-geophysical approach: The Quesnel Forks landslide, Landslides, 1, 1, 29-40, doi:10.1007/s10346-003-0008-7.

Cárdenas-Soto, M., J. Sánchez-González, J. A. Martínez-González, D. Escobedo-Zenil et al. (2024). A combination of seismic refraction and ambient noise methods to detect landslide-prone materials, Geophys. Int., 63, 3, doi:10.22201/igeof.2954436xe.2024.63.3.1585.

Chávez-García, F. J., T. Natarajan, M. Cárdenas-Soto and D. Escobedo-Zenil (2020). Landslide characterization using active and passive seismic imaging techniques: A case study from Kerala, India, Nat. Haz., doi:10.22201/igeof.2954436xe.2024.63.3.1585.

Cruden, D. M. and D. J. Varnes (1996). Landslide types and processes, in Landslides: investigation and mitigation, Transportation Research Board, National Research Council, Special Report, A. K. Turner and R. L. Schuster (Eds.), 247, National Academy Press, Washington DC, 36-75.

Del Gaudio, V., S. Muscillo and J. Wasowski (2014). What we can learn about slope response to earthquakes from ambient noise analysis: an overview, Eng. Geol., 182, 182-200, doi:10.1016/j.enggeo.2014.05.010.

Foti, S., C. G. Lai, G. J. Rix and C. Strobbia (2014). Surface wave methods for near-surface site characterization, CRC Press, doi:10.1201/b17268.

Harba, P., Z. Pilecki and K. Krawiec (2019). Comparison of MASW and seismic interferometry with use of ambient noise for estimation of S-wave velocity field in landslide subsurface, Acta Geophys., 67, 6, 1875-1883, doi:10.1007/s11600-019-00344-9.

Highland, L. M. and P. Bobrowsky (2008). The landslide handbook-A guide to understanding landslides, Circular, 1325, U.S. Geological Survey, Reston, Virginia, ISBN:978-141132226-4.

Hungr, O., S. Leroueil and L. Picarelli (2014). The Varnes classification of landslide types, an update, Landslides, 11, 167-194, doi:10.1007/s10346-013-0436-y.

Hussain, Y., O. Hamza, M. Cárdenas-Soto, W. R. Borges et al. (2020). Characterization of Sobradinho landslide in fluvial valley using MASW and ERT methods, REM, Int. Eng. J., 73, 487-497, doi:10.1590/0370-44672019730109.

Imani, P., G. Tian, S. Hadiloo and A. Abd El-Raouf (2021). Application of combined electrical resistivity tomography (ERT) and seismic refraction tomography (SRT) methods to investigate Xiaoshan District landslide site: Hangzhou, China, J. Appl. Geophys., 184, 104236, doi:10.1016/j.jappgeo.2020.104236.

Jaafari, A. (2024). An overview of triggering and causing factors of landslides, in Landslides in the Himalayan Region: Risk Assessment and Mitigation Strategy for Sustainable Management U. Chatterjee, K. C. Lalmalsawmzauva, B. Biswas and S. C. Pal (Eds.), 25-45.

Jongmans, D. and S. Garambois (2007). Geophysical investigation of landslides: a review. Bulletin de la Société Géologique de France, 178, 2, 101-112, doi:10.2113/gssgfbull.178.2.101.

Kjekstad, O. and L. Highland (2009). Economic and social impacts of landslides, in Landslides Disaster Risk Reduction K. Sassa and P. Canuti (Eds.), Springer, 573-587, doi:10.1007/978-3-540-69970-5_30.

Mauritsch, H. J., W. Seiberl, R. Arndt, A. Römer et al. (2000). Geophysical investigations of large landslides in the Carnic Region of southern Austria, Eur. J. Environ. Eng. Geophys., 5, 3, 143-156, doi:10.1007/PL00013716.

Pazzi, V., S. Morelli and R. Fanti (2019). A review of the advantages and limitations of geophysical investigations in landslide studies, Int. J. Geophys., 1, 2983087, doi:10.1155/2019/2983087.

Petley, D. (2012). Global patterns of loss of life from landslides, Geology, 40, 10, 927-930, doi:10.1130/G33217.1.

Rahimi, S., T. Moody, C. Wood, B. Mofarraj Kouchaki et al. (2019). Mapping subsurface conditions and detecting seepage channels for an embankment dam using geophysical methods: A case study of the Kinion Lake Dam, J. Environ. Eng. Geophys., 24, 3, 373-386, doi:10.2113/JEEG24.3.373.

Rahimi, M., C. M. Wood and K. M. Befus (2024a). Estimation of Sediment Depth for a Dam Removal Project Using Combined Underwater and Land Electrical Resistivity Tomography (ERT), in Geo-Congress 2024, 585-593, doi:10.1061/9780784485309.060.

Rahimi, M., C. M. Wood and L. F. Kallivokas (2024b). A comparative study of using geophysical methods for imaging subsurface voids of various sizes and at different depths, Eng. Geol., 341, 107711, doi:10.1016/j.enggeo.2024.107711.

Rahimi, S., C. M. Wood and M. Bernhardt-Barry (2021). The MHVSR technique as a rapid, cost-effective, and noninvasive method for landslide investigation: case studies of Sand Gap and Ozark, AR, USA, Landslides, 18, 8, 2705-2720, doi:10.1007/s10346-021-01677-7.

Samodra, G., M. F. Ramadhan, J. Sartohadi, M. A. Setiawan et al. (2020). Characterization of displacement and internal structure of landslides from multitemporal UAV and ERT imaging, Landslides, 17, 10, 2455-2468, doi:10.1007/s10346-020-01428-0.

Sebastiano, D., P. Francesco, M. Salvatore, I. Roberto et al. (2019). Chapter 12 – Ambient noise techniques to study near-surface in particular geological conditions: A brief review, in Innovation in Near Surface Geophysics R. Persico, S. Piro and N. Linford (Eds.), Elsevier, 419-460, doi:10.1016/B978-0-12-812429-1.00012-X.

SESAME European Research Project (2004). Guidelines for the implementation of the H/V spectral ratio technique on ambient vibration: Measurements, processing and interpretations, Project No. EVG1-CT-2000-00026.

Uhlemann, S., J. Chambers, P. Wilkinson, H. Maurer et al. (2017). Four-dimensional imaging of moisture dynamics during landslide reactivation, J. Geophys. Res. Earth Surf., 122, 1, 398-418, doi:10.1002/2016JF003983.

Whiteley, J. S., J. E. Chambers, S. Uhlemann, P. B. Wilkinson et al. (2019). Geophysical monitoring of moisture-induced landslides: A review, Rev. Geophys., 57, 1, 106-145, doi:10.1029/2018RG000603.

Yust, M. B., B. R. Cox, J. P. Vantassel and P. G. Hubbard (2024). DAS for 2-D MASW imaging: a case study on the benefits of flexible subarray processing, Geophys. J. Int., 237, 3, 1609-1623, doi:10.1093/gji/ggae122.

Zywicki, D. J. and G. J. Rix (1999). Frequency-wavenumber analysis of passive surface waves, in Symposium on the Application of Geophysics to Engineering and Environmental Problems, Society of Exploration Geophysicsts, 75-84, doi:10.4133/1.2922675.

***CORRESPONDING AUTHOR: Clinton WOOD**,
University of Arkansas, Civil engineering faculty, Fayetteville, AR, USA
e-mail: cmwood@uark.edu